Integrated Impedance-Matching Coupler for Smart Building and Other Power-Line Communications Applications

Petrus A. Janse van Rensburg, *Member, IEEE*, Mloyiswa P. Sibanda,
and Hendrik C. Ferreira, *Senior Member, IEEE*

***Abstract* — Power-line communications is a promising technology to help automate buildings, as it utilizes the in-situ power cabling as a communications channel. However, couplers are required to inject and extract the communication signal from the power grid. Most power-line communications couplers make use of a small transformer to adapt impedance levels while also providing galvanic isolation. The cost and size of these transformers have been hindrances in the quest for compact, economic couplers. Previous attempts to eliminate this coupling transformer, while maintaining impedance adaptation, have not been successful in reducing component cost nor physical size. In this paper, a novel approach is followed: (1) a suitable dual-function band-pass matching circuit is designed as for ordinary electronics, whereafter (2) the specifications of this band-pass matching circuit is upgraded to function safely in the power-grid environment as a coupler. Therefore a matching circuit is transformed into a compact power-line coupler, which further exhibits band-pass filtering and excellent impedance-adapting performance. Simulations as well as laboratory measurements are shown which confirm the accuracy of the design. Finally, practical 220-V measurements in an office block are presented, which prove the versatility of this novel coupler when power-grid conditions fluctuate.[1]**

***Index Terms* — Power system communications, home automation, coupling circuits, impedance matching, filtering.**

I. Introduction

ALTHOUGH power-line communications (PLC) has been studied for decades, PLC coupling has been a neglected topic, and has only received new attention during the past few years [1]-[9]. Some investigations regarding peripheral issues and comparative performance of couplers have been made, e.g. [7]-[9], however proper analysis and design of couplers themselves has been limited, see [1]-[6].

Amongst other applications, PLC is also being investigated and developed as a promising technology to help automate homes and other buildings without having to pay for network cabling [10]-[15]. However, to inject and/or extract the communication signal into- and from the in-situ power cabling, PLC couplers are required. These couplers may be as simple as a single series capacitor, however, the majority of capacitive couplers have an added coupling transformer for galvanic isolation and impedance adaptation [1]-[6], [16]-[19]. It is this coupling transformer that dominates the cost of power-line communications couplers, as the core, copper conductors, and manufacturing costs are expensive.

Coupling and impedance adaptation without the industry-standard coupling transformer, has been the topic of investigation in [20] and [21], respectively. However, for this cascaded two-stage solution, complexity and component count had risen to unacceptable levels – see Fig. 1(a).

As a novel solution, in this paper a band-pass impedance matching circuit is thus proposed, which consists of only two inductors and two capacitors, and which is further upgraded to function as a PLC coupler. However, after integration of the inductive part of the power-line impedance into the circuit, only three components are required – see Fig. 1(b).

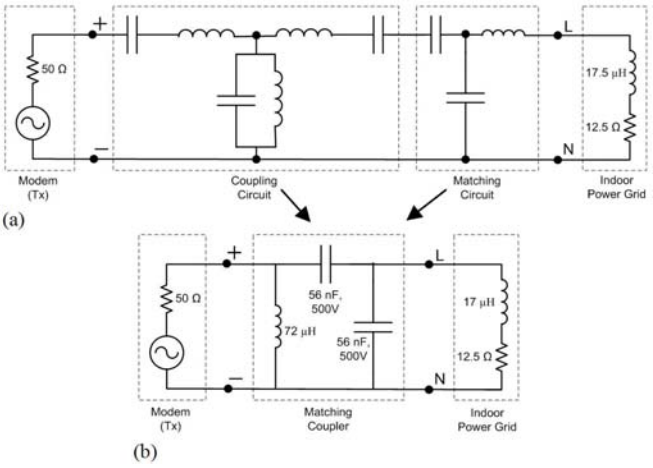

Fig. 1. 'Before and after' circuit diagrams comparing complexity and component count. (a) Cascaded band-pass coupler and impedance matching circuit [18]. (b) Novel matching coupler.

In the sections to follow, the design of a basic 4-element band-pass matching circuit is presented (Section II). Next, Section III discusses requirements imposed on such a matching circuit by the demanding power-line environment – to function properly as a coupler. Following this, simulation results and laboratory measurements are compared in Section IV. Finally, practical 220-V power-line measurements in an office block are presented in Section V. These measurements show excellent performance at the impedance level which the coupler was designed for. However, even at various lower and

[1] This work was supported in part by the South-African utility company ESKOM's TESP Programme, as well as the National Research Foundation (Grant UID 85320).

P. A. Janse van Rensburg and M. P. Sibanda are with Walter Sisulu University, East London, South Africa (email pvanren@wsu.ac.za and msibanda@wsu.ac.za). H. C. Ferreira is with University of Johannesburg, South Africa (email hcferreira@uj.ac.za).

higher power-line impedance levels, the prototype coupler performed well, yielding many decibels of improvement over each mismatch level.

II. Design of Band-pass Matching Circuit

In the design of this prototype only lumped parameters are used as the frequency of operation is 110 kHz. For broadband PLC (> 1 MHz), parasitic effects would play a more important role and should thus be included in the modeling and design. For relevant impedance matching background theory and how it relates to power-line communications, the reader is referred to [1]-[5], [16]-[19] but specifically also [21]-[23], where the basic building block of impedance matching circuits (the L-Section) is discussed. These impedance matching L-Sections can effect either a high-pass or a low-pass filter circuit, depending on configuration of inductors and capacitors. However, a band-pass impedance matching circuit may be constructed by utilizing two cascaded L-Sections, where one effects a high-pass response, the other a low-pass response, and thus the two in cascade, yield a band-pass filter. Two topologies are possible, depending on the order of the low-pass and high-pass L-Sections. The choice between the two topologies, may be determined by various factors and is discussed in Section V. However, the design of such a band-pass ladder network is considered first.

A 50-Ω modem to 12.5-Ω power line (resistive) mismatch, and associated 4-element matching band-pass ladder-network is shown in Fig. 2. Typical indoor *R-L* power-line network impedance values of 12.5 Ω and 17.5 µH are assumed for frequencies below 500 kHz, since these parameters usually vary between 5 Ω and 20 Ω (resistive) as well as 7 µH to 27 µH (inductive) – see [16]. To simplify the design process and facilitate laboratory testing (Section IV), the resistive part of the power-line impedance will be considered first, however the inductive part will be incorporated into the design later (see Section V).

The design steps for such a matching network (shown in Fig. 2) make use of similar concepts as is used for L-Sections [21]-[23]. However, a virtual shunt resistor is introduced between the two L-sections to help facilitate the design, by breaking the design up into two stages. Thus the left hand side and the right hand side of the circuit in Fig. 2, will both be matched to the value of this virtual resistor, yielding a compatible, matched circuit.

Also, the value of the virtual resistor (acting as an in-between stage) has to be between the two extremes of the source and load impedance. Furthermore, the widest pass-band (lowest Q-factor) for matching can be obtained by choosing the virtual resistor R_V equal to the geometric mean of the two terminal impedances [22], i.e.

$$R_V = \sqrt{R_S \cdot R_P}\,, \tag{1}$$

R_S being the series transmitter output impedance, and R_P representing the parallel 'receiver' (here power-line) input impedance.

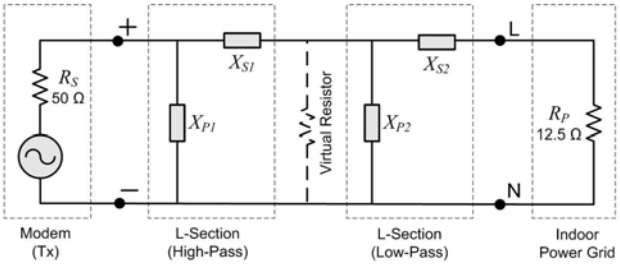

Fig. 2. Band-pass matching ladder network, made up of two cascaded L-Sections, one high-pass and one low-pass. A virtual resistor is inserted only for the design, in order to break the design up into two stages.

Therefore, assuming a 50-Ω to 12.5-Ω (resistive) impedance mismatch between the communication system and the power-line network, $R_V = [(50)(12.5)]^{1/2} = 25$ Ω. Once R_V has been defined, the rest of the calculations follow similar steps to those outlined in [21]. For the L-section with the larger terminating impedance (a typical 50-Ω modem impedance), the quality factor is defined by:

$$Q_S = \sqrt{\frac{R_S}{R_V} - 1} = \sqrt{\frac{50}{25} - 1} = 1\,. \tag{2}$$

For the L-section with the smaller termination impedance (in this case a typical 12.5-Ω indoor power-line resistance), the Q-factor is defined by:

$$Q_P = \sqrt{\frac{R_V}{R_P} - 1} = \sqrt{\frac{25}{12.5} - 1} = 1\,. \tag{3}$$

Because quality factor can also be expressed as ratio of reactance to resistance [21]-[23]:

$$Q_S = X_S / R_S \quad \text{(for series branches) and} \tag{4}$$

$$Q_P = R_P / X_P \text{ (for parallel branches),} \tag{5}$$

the following design steps may be followed to obtain reactance values for Fig. 2.

For the first L-section, calculate the required reactance of the series branch using (4), $X_{S1} = Q \cdot R_V = (1) \cdot (25) = 25$ Ω. For the first L-section, also calculate the reactance of the parallel branch using (5), $X_{P1} = R_S/Q = (50)/(1) = 50$ Ω. For the second L-section, calculate the reactance of the series branch using (4), $X_{S2} = Q \cdot R_S = (1) \cdot (12.5) = 12.5$ Ω. Lastly, for the second L-section, calculate the reactance of the parallel branch using (5), $X_{P2} = R_V/Q = (25)/(1) = 25$ Ω.

The above calculations yield the required reactance values for a 50-Ω to 12.5-Ω 4-element band-pass matching network (see Fig. 2). Two realizations are possible, depending on the chosen topology of capacitors and inductors. See Fig. 3 (a) and (b) of which the former proved to be more suitable – refer to Section V for a discussion. Given the center frequency f_C = 110 kHz, capacitor values can be obtained using:

$$C = \frac{1}{2\pi \cdot f_C \cdot X}\,, \tag{6}$$

while the inductor values may be calculated using:

$$L = \frac{X}{2\pi \cdot f_C}\,. \tag{7}$$

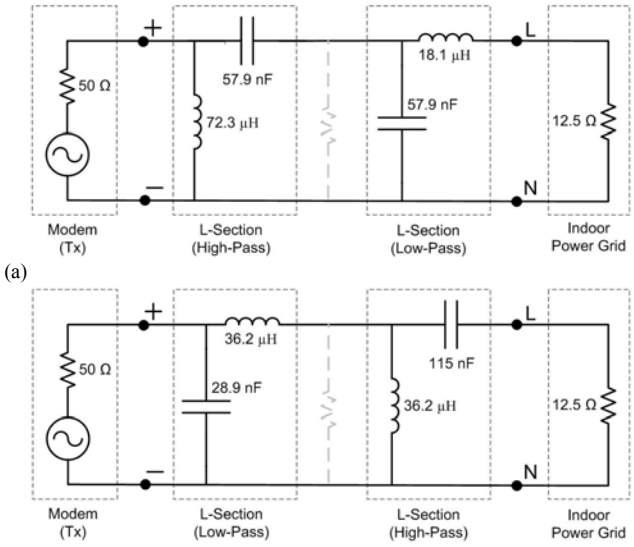

Fig. 3. Two possible realization options for the band-pass impedance matching network (50-Ω and 12.5-Ω terminal impedances) with *L* and *C* components for a center frequency of 110 kHz.

Next, the specifications of these components still have to be adapted for the power-line environment in order to use it as a PLC coupler.

III. Upgrading the Band-pass Matching Circuit to a Power-Line Coupler

The required modem maximum output current specification can be obtained by setting the power-line impedance to zero in Fig. 3(a) – in case a fault occurs on the power-line side. Apart from impedance matching, another important task of this novel PLC coupler, is to sufficiently filter the power waveform for two reasons: (i) In order that the modem electronics is not damaged (for this reason the remainder of the power waveform after filtering has to be below say 20 volts peak), and (ii) in order that the input of the receiver is not saturated, causing the received signal to be distorted. Acceptable, filtered, power waveform peak voltage levels (to prevent receiver saturation) would differ from design to design, but should preferably be below 1 volt (peak). Therefore sufficient filtering of the 50-Hz waveform should be confirmed, after the impedance matching circuit has been designed – see below.

For a 240-V_{RMS} residential power grid, a peak voltage of ~340 V may be experienced, and capacitors with a 500-V blocking voltage are typically used for such applications. To make recommendations for coupler component specifications however, it is best to consider impedance (reactance) values at power waveform frequencies. Fig. 4 shows an equivalent circuit for Fig. 3(a) at 50 Hz.

To consider the effect of the 50-Hz power waveform on the coupler and modem electronics, the circuit needs to be considered in reverse mode, pretending that the modem now 'receives' this 'transmitted' waveform. If a worst-case 50-Hz, 340-V peak voltage is resident between live and neutral outlets (Fig. 4), it is evident that the series 5.7-mΩ inductive reactance is effectively a short circuit and has almost no influence, thus the voltage divider rule predicts that practically the entire 340 V would appear across the parallel capacitor (Fig. 4). Therefore this capacitor needs to be rated as a 500-V capacitor.

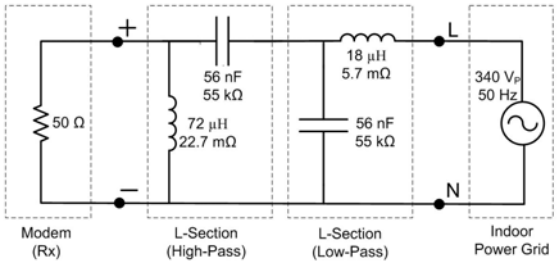

Fig. 4. Reactance values of Fig. 3(a) at a 50-Hz power-line waveform frequency. For worst-case calculations, an ideal power-line source with zero impedance is assumed. Circuit is considered in reception mode with modem voltage source short-circuited.

Next, the parallel 72.3 μH inductance (Fig. 4) is considered, which is also effectively a short circuit (22.7 mΩ) at 50 Hz, thus clamping the 50-Hz voltage across the modem to almost zero. This low-frequency effect is part of the combined filtering action of this circuit, which yields a band-pass response as is shown in Section IV. In a worst-case scenario, the voltage divider rule predicts that its 22.7-mΩ reactance would only experience a ratio (22.7 mΩ)/(55 kΩ + 22.7 mΩ) of the peak 340 volts, i.e. only approximately 140 μV (peak) across itself and thus also across the parallel modem input. In case of a default at modem input (i.e. short circuit), zero volts would be present across this inductor, and the same above requirements are still applicable. Thus the matching coupler would function effectively in reducing the power waveform to a safe and acceptable level.

The remaining 50-Hz voltage (essentially 340 V_{PEAK}) would be dropped across the series capacitor, which thus helps to effect the filtering action of the PLC coupler. Therefore this series capacitor also has to be rated 500 V. Further, the frequency response of each capacitor needs to be satisfactory, with a stable capacitance for frequencies within the required pass-band of the PLC coupler.

For the specific circuit in Fig. 4, the two inductors have minimal current and voltage rating requirements, but do need to be stable versus frequency, especially within the communication band. For coupler circuits where inductors carry larger currents, conductors have to be adequate, and care must be taken to ensure that the inductor core does not saturate at low power-waveform frequencies.

To compare cost and size of this novel matching coupler with a traditional transformer-capacitor coupler (Fig. 5), quotations for the applicable components were obtained [24]. Compare Table I with Table II which show that only a marginal size reduction is achieved, however a substantial cost reduction is possible with the new coupler.

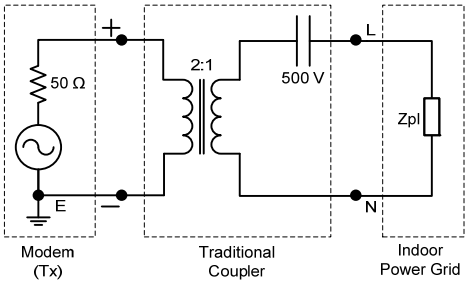

Fig. 5. Traditional transformer-capacitor coupler used as a benchmark for cost and performance.

TABLE I
COST AND PCB FOOTPRINT SIZE – TRANSFORMER COUPLER

Component and Specification	Cost ($US) @MOQ 10,000	PCB Footprint (mm^2)
1 x Capacitor 1 μF/400 V	$0.153	4 x 13 = 52 mm^2
1 x Transformer PLC/ADSL	$0.973	12 x 12 = 144 mm^2
Total: Transformer Coupler	**$1.126**	**196 mm^2**

TABLE II
COST AND PCB FOOTPRINT SIZE – MATCHING COUPLER (SEE FIG. 9)

Component and Specification	Cost ($US) @MOQ 10,000	PCB Footprint (mm^2)
2 x Capacitor 56 nF/400 V	$0.140 each	4 x 13 = 52 mm^2 each
1 x Inductor 72 μH	$0.329	5.5 x 15 = 82.5 mm^2
Total: Matching Coupler	**$0.609**	**186.5 mm^2**

IV. LABORATORY VS. SIMULATION RESULTS

In this section, the performance of the designed matching coupler is evaluated by simulation and experimental measurements. In order to confirm band-pass filtering and impedance matching, the transfer function of the designed circuit (Fig. 3(a)) was simulated on computer. A prototype was also constructed to confirm band-pass filtering and matching experimentally.

To test the prototype in the laboratory, a Goldstar FG2002C signal generator (acting as a transmitter) was swept through the frequencies under consideration, while an IFR2397 spectrum analyzer measured the received signal strength, using the maximum hold function. The matching coupler prototype was the only circuitry between above transmitter and receiver instruments.

The variable power-line (receiver) resistance was emulated by paralleling a specific number of calibrated 50-Ω terminations with the internal instrument impedance of 50 Ω. For example, 3 external 50-Ω terminations added to the internal 50-Ω spectrum analyzer impedance, yields ~12.5 Ω (resistive) – see Fig. 6(a). Multiple laboratory tests and simulations were performed to check the performance of the 50-Ω to 12.5-Ω matching coupler under fluctuating power-line impedance conditions.

Experimental confirmation of the new coupler's band-pass filtering (linear scale) is shown in Fig. 6(b) as well as improved impedance matching of ~2 dB, given a 50-Ω to 12.5-Ω mismatch level as base line. Also, if the power-line impedance drops by 50 % to 6.25 Ω, the general purpose matching coupler still achieves gains of roughly 4 dB over the mismatch base line.

The simulation results for loads of 12.5 Ω and 6.25 Ω are shown in Fig. 6(c), again benchmarked against the appropriate mismatch level. Although designed for the typical (12.5-Ω resistive) indoor power grid, various simulation results showed that the 50-Ω to 12.5-Ω matching coupler circuit still provides significant gains when used with incorrect terminating power-line impedances.

(a)

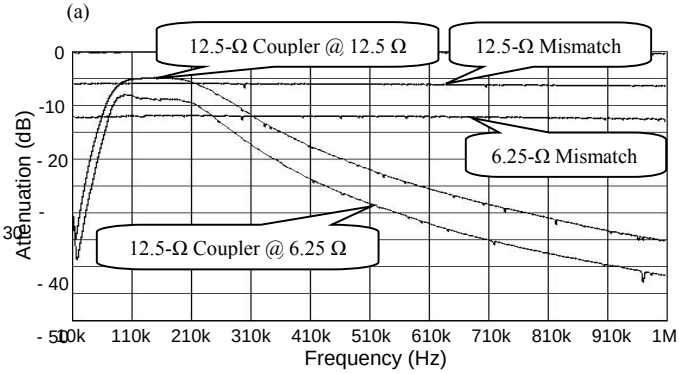

(b)

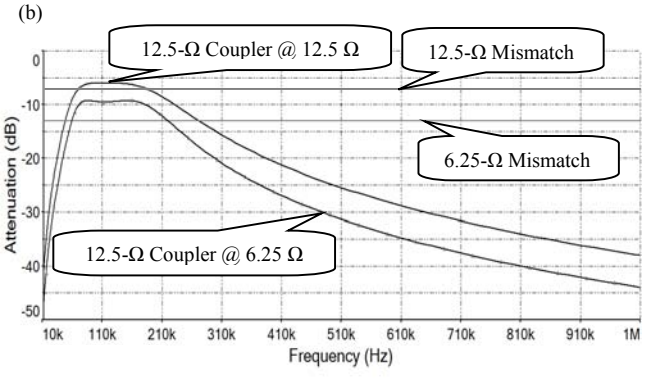

(c)

Fig. 6. (a) External 50-Ω terminations in parallel with an instrument input impedance to emulate a 12.5-Ω power-line resistance. (b) Band-pass response of the prototype (linear scale) and ~2 dB of gain realized by the matching coupler compared to the measured mismatch base line. (c) Simulation results confirming measured results in (b). The top curve shows the matching coupler response for the correct (matched) 12.5-Ω load. However, if used to couple an incorrect 6.25-Ω load (bottom curve), ~4 dB is still gained over the mismatch level.

The versatility of the matching coupler in the above measurements and simulations, raised the question of how the prototype would compete against a correctly matched coupler for a power-line impedance lower than 12.5 Ω. Therefore the lowest (most severely loaded) power-line condition of 3.125 Ω was investigated by means of simulation. These results are shown in Fig. 7 which contrasts the response when using a correctly matched 3.125-Ω coupler, against the (now unmatched) 12.5-Ω prototype coupler.

Interestingly, the simulation response shows that a correctly matched coupler (for 3.125-Ω power line load) will provide only approximately 3 dB of gain over the prototype general-purpose matching coupler (which was designed for 12.5 Ω). Also, a fairly flat response within pass-band is shown by the 3.15-Ω coupler compared to the prototype general-purpose coupler which dips inside the pass band. A narrower pass-band and somewhat improved filtering are also shown by the correctly matched coupler.

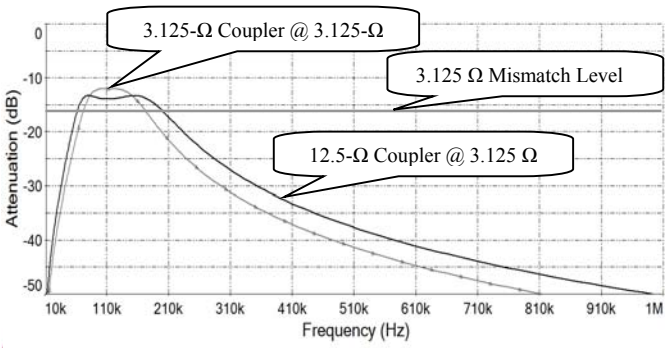

Fig. 7. Simulated comparison of matched 3.125-Ω coupler response and 12.5-Ω (general purpose) coupler response for a 3.125-Ω power-line load. Only ~3 dB is sacrificed when using the 12.5-Ω general-purpose coupler.

V. Practical Results

In order to test the practical performance of the proposed band-pass matching coupler, two prototype 50-ohm to 12.5-ohm matching coupler circuits were built with specifications to withstand the strain of the 220-V_{RMS} power grid. The two couplers were used as a transmitter-receiver coupler pair, with the live power-line channel in between. Fig. 8 illustrates the measurement setup that was used to test the practical performance of these matching couplers.

The two matching couplers were constructed according to Fig. 3(a), however an important change was made. Upon considering which topology to implement – Fig. 3(a) vs. Fig. 3(b) – it was discovered that the first configuration allows the incorporation of the typical power-line inductance into the matching circuit, as was done for practical measurements in this section.

Take note that the matching procedure used in the design of Fig. 3(a) assumed resistive terminal impedances. As such, only the typical power-line resistance was taken into account, however, the power-line inductance was not. If the matching coupler of Fig. 3(a) is used, the power-line inductance can now form part of the solution, to help implement the matching circuit.

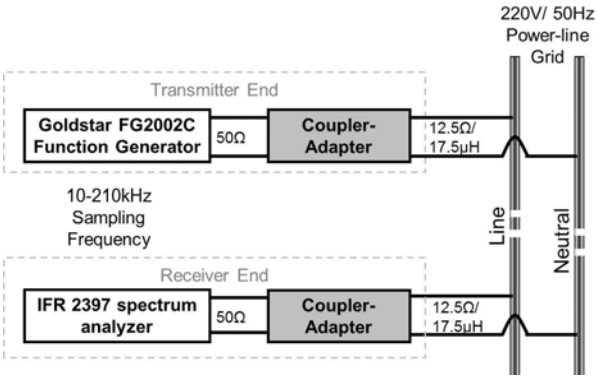

(a)

(b)

Fig. 8. (a) Schematic representation and (b) photos of the live measurement setup used to test the performance of the matching couplers in an office block.

The expected 17.5-μH power-line inductance was sufficiently close to the design value of 18 μH, so that the role of this component could be fulfilled by the power-line inductance. In previous designs, the value of this required series inductor was merely reduced by the value of expected power-line inductance (as the two in series would make up the required total) – see [21]. Fig. 9 shows the final prototyped coupler, where the typical power-line inductance is utilized to help fulfill filtering and matching functions, and thus a three-element matching coupler results.

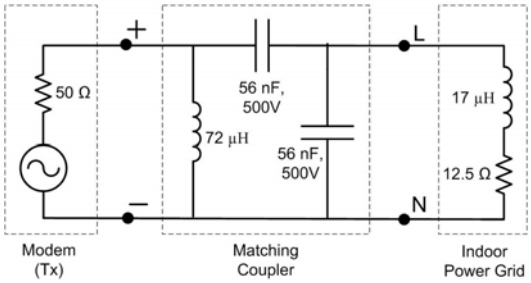

Fig. 9. Prototyped 50-Ω to 12.5-Ω matching coupler for practical deployment. Only 3 components are required for the coupler, as the power-line inductance fulfills the function of the fourth.

The practical test results below were carried out in an office block (see Fig. 10) and show the performance of the prototyped matching couplers compared to standard transformer-couplers (a pair of 1:1 transformer-couplers and another pair of 2:1 transformer-couplers). In [2] it was shown that a 2:1 transformer-coupler makes a good general-purpose coupler for average distances between modem and dominating load (and 50-Ω modems). See Fig. 11. Thus the performance

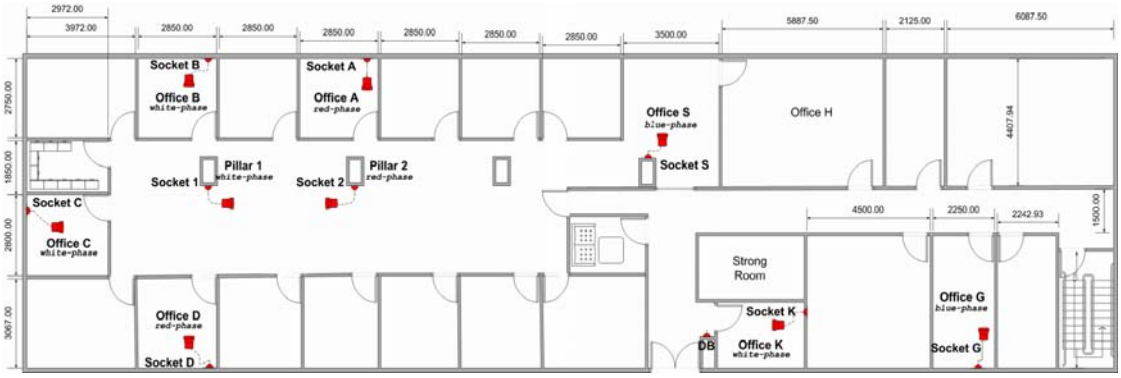

Fig. 10. Office block floor plan showing power terminals and various Tx-Rx routes used during practical tests.

of the matching coupler was compared with this benchmark provided by a 2:1 transformer-coupler. Also take note that a 1:1 transformer coupler provides no impedance matching, but is useful as it provides a reference curve for the practical measurements which follow below.

The first set of measurements were carried out between Office A and Office D (see Fig. 10), both connected to the red phase in a three-phase office block distribution network. A socket in-between the two offices (Pillar 2) was used as a central loading point to mimic conditions for the loading-vs-distance model in [2]. The dominating load (in this case additional loads) should be midway between two modems for the two modems to require identical winding ratios [2]. A 4600-W load, equivalent to ~10.5 ohms, was used as an additional load at Pillar 2 (Fig. 10).

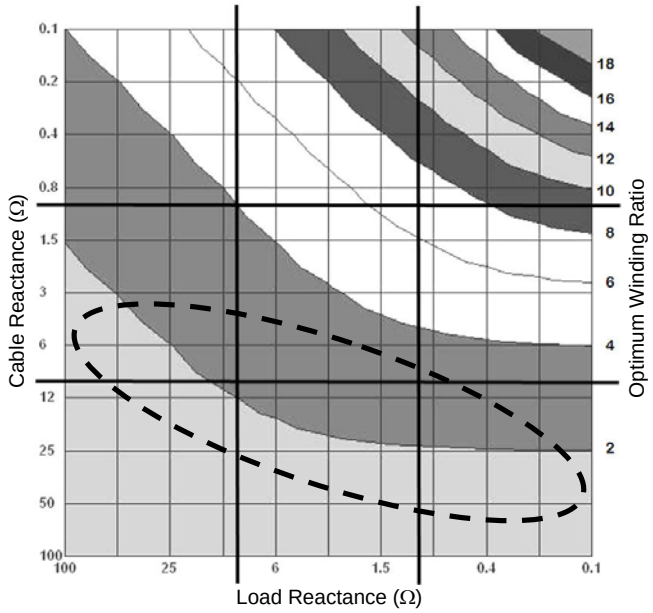

Fig. 11. Optimum winding ratio contours for a transformer-coupler from [2]. Y-axis represents distance while X-axis represents loading. Dashed ellipse indicates area where general-purpose 2:1 transformer-coupler will yield good results.

This first set of practical results is shown in Fig. 12 – for frequencies up to ~1 MHz so that the prototype coupler's band-pass filter effect can be seen. The novel band-pass coupler shows improved filtering out of band, however noise within the pass-band would still enter a modem when the coupler is used in receiving mode. Take note that improved intra-band reception increases both signal levels and received noise levels by the same factor and thus does not alter the received signal-to-noise ratio. As for all modems, internal circuitry still has to distinguish between signal and noise.

For narrowband PLC frequencies below 300 kHz in Fig.12, the new prototype coupler pair performed on par, and even outperformed the traditional 2:1:2 coupler pair. Within the pass-band region, impedance matching further provided gains of up to ~8 dB over a 1:1:1 transformer-coupler pair.

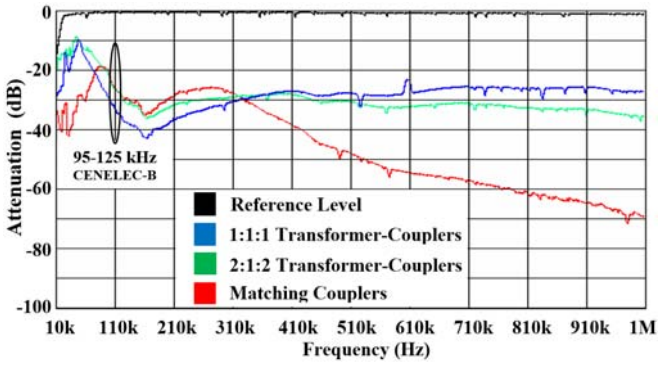

Fig. 12. Practical 220-V measurement results (Office A – D) to show band-pass filtering provided by prototype coupler pair. At 110 kHz, both the matching coupler pair and 2:1:2 transformer-coupler pair yielded ~26 dB attenuation compared to the ~33 dB reference of the 1:1:1 transformer-coupler pair.

Next, measurements were taken between two offices (Office B and Office K, Fig. 10) – both connected to the white phase of the three-phase indoor office network. A socket at Pillar 1 was used as a loading point to mimic the model in [2]. By varying loads at such a central point, one can move the operating point along the horizontal X-axis in Fig. 11, thus impacting on optimum impedance matching required. These effects can be seen in Fig. 13 and Fig. 14 which show practical 220-V results up to 210 kHz between Office B and Office K.

Results with no additional loads at Pillar 1, is shown in Fig. 13 while Fig. 14 shows results with additional loads of ~10.5

ohms connected at Pillar 1. Without additional loading (Fig. 13), the prototype matching coupler pair outperformed the traditional 2:1:2 transformer-coupler pair by ~2 dB, and also the 1:1:1 transformer-coupler pair by a large ~8 dB, at 110 kHz.

With additional loading (Fig. 14) the prototype matching coupler pair performs even better within the pass-band. At 110 kHz, the new matching coupler pair outperforms the traditional 2:1:2 transformer-coupler pair by ~5 dB. However, it provides as much as ~12 dB of gain, compared to the base-line performance of the 1:1:1 transformer-coupler pair.

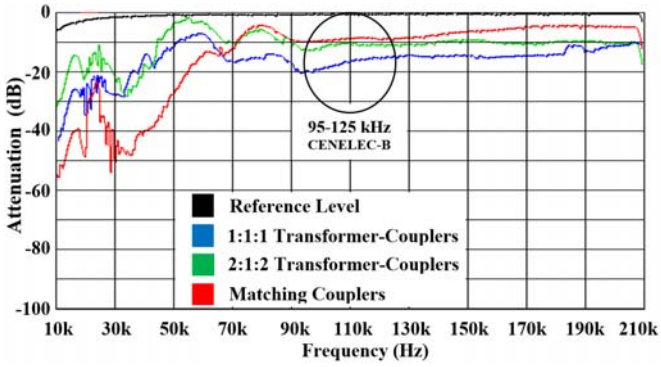

Fig. 13 Practical 220-V measurements (Office B – Office K) without additional loads. At 110 kHz the matching coupler pair yielded only ~9 dB of attenuation compared to the 2:1:2 transformer-coupler pair's ~11 dB and the 1:1:1 transformer-coupler pair's ~17 dB of attenuation.

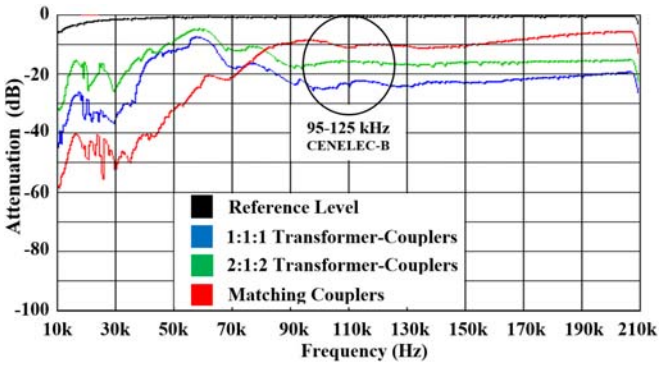

Fig. 14 Practical 220-V measurements (Office B – Office K) with additional loads (~10.5 Ω @ 50 Hz) connected to the indoor power-line network (Pillar 1). At 110 kHz, the matching coupler pair outperforms the 2:1:2 and 1:1:1 transformer-coupler pairs by ~5 dB and ~12 dB respectively.

Take note that the measured curves in Fig. 12, Fig. 13 and Fig. 14 are effectively transfer functions measured between various live power outlets in an office block. These curves thus display the effect of the cabling, branching and loads between transmitter and receiver points, combined with the filtering and matching of the coupler as was measured in Section IV.

Apart from the shown practical measurements, various other transmission paths and loading scenarios were investigated. These measurements confirmed that the new matching coupler pair in most cases performed on par, or outperformed the traditional general-purpose 2:1:2 transformer coupler pair.

The main reason is that both coupler types cater for resistive / modulus mismatches, however the matching coupler further caters for the reactive part of the mismatch. Although this power-line reactance does fluctuate with changes in location, frequency, and time (and may even become capacitive), the prototype was designed for average conditions. The main reason for this approach, is that the end goal of the prototype coupler was to be an economical, static coupler – and not an adaptive coupler which requires control circuitry and would thus be more expensive. As the power-line inductance deviates from the static design average, gains offered by the matching coupler will thus be reduced. However, in most cases improved matching will take place, compared to traditional transformer (modulus) matching – which does not cater for reactive components of the power-line impedance. Similar to the simulation results, the presented practical results also confirmed the versatility of the new matching coupler for various time-fluctuating power-line load levels.

VI. Conclusion

A relatively expensive and bulky component of traditional PLC couplers, is the coupling transformer, which adapts impedance levels between modem and power grid. Previous attempts to save costs by eliminating this coupling transformer were not particularly successful. In this paper, a novel approach was presented, which yielded a compact coupling circuit that fulfils numerous functions: coupling (safety), band-pass filtering, and impedance matching. Even the inductive part of the indoor power-line impedance was integrated into the design, reducing component count further.

Although the novel matching coupler was designed for average indoor impedance levels, simulations and laboratory tests showed improved performance even when power-line impedance levels fluctuate. Practical, indoor 220-V measurements further confirmed the versatility of the coupler, which outperformed a general-purpose 2:1 transformer coupler in most cases. One limitation of the novel PLC coupler, is that galvanic isolation is not achieved. Thus for safety reasons the proposed coupler should either interface with the modem via differential (non-earthed) inputs/outputs, or alternatively be deployed in double-insulated packaging.

Although this project was aimed at narrowband, smart building type PLC applications, the above design principles can easily be extrapolated for outdoor narrowband smart grid PLC applications where impedance levels are also roughly linear against frequency, but at lower levels than for indoor cases, see [25]-[27].

However, the access impedance of broadband PLC networks (> 1 MHz) are typically more frequency selective, and vector fitting may be necessary to match the impedance over the required frequency response range, see e.g. [28]. This will result in more passive components, and the typical cost-

versus-performance tradeoff would have to be considered. Also, at these higher frequencies, various parasitic effects (especially capacitive effects) may have to be considered, as lumped parameter modeling may not be sufficient any more.

REFERENCES

[1] P. A. Janse van Rensburg, H. C. Ferreira, "Design of a bidirectional impedance-adapting transformer coupling circuit for low-voltage power-line communications," *IEEE Trans. on Power Delivery*, vol. 20, no. 1, Jan. 2005, pp. 64-70.

[2] P. A. Janse van Rensburg, H. C. Ferreira, "Coupler winding ratio selection for effective narrow-band power-line communications," *IEEE Trans. on Power Delivery*, vol. 23, no. 1, Jan. 2008, pp. 140-149.

[3] P. A. Janse van Rensburg, H. C. Ferreira, "Design and Evaluation of a Dual Impedance-Adapting Power-Line Communications Coupler," *IEEE Trans. on Power Delivery*, vol. 25, no. 2, Apr. 2010, pp. 667-673.

[4] P. A. Janse van Rensburg, "Chapter 4: Coupling," in *Power-Line Communications*, ed. H. C. Ferreira, L. Lampe, J. Newbury, T. G. Swart, John Wiley & Sons Ltd., Chichester, 2010, p.147-194.

[5] P. A. Janse van Rensburg, A. J. Snyders, H. C. Ferreira, "Complementary capacitive-inductive data coupler for power-line communications," *Australian Patent*, No. 2011101421, sealed 24 Nov. 2011.

[6] P. A. Janse van Rensburg, H. C. Ferreira, "Coupling circuitry: understanding the functions of different components," in *Proc. 7th Int. Symp. Power-Line Comm.*, 2003, pp. 204-209.

[7] J. Nguimbis, S. Cheng, Y. Zhang, L. Xiong, "Coupling unit topology for optimal signaling through the low-voltage powerline communication network," *IEEE Trans. on Power Delivery,* vol. 19, no. 3, Jul. 2004, pp. 1065-1071.

[8] P. A. A. F. Wouters, P. C. J. M. Van der Wielen, J. Veen, P. Wagenaars, E. F. Steennis, "Effect of cable load impedance on coupling schemes for MV power line communication," *IEEE Trans. on Power Delivery,* vol. 20, no. 2, Apr. 2005, pp. 638-645.

[9] G. A. Franklin, "A Practical Guide to Harmonic Frequency Interference Affecting High-Voltage Power-Line Carrier Coupling Systems," *IEEE Trans. on Power Delivery,* vol. 24, no. 2, Apr. 2009, pp. 630-641.

[10] C. J. Kim, M. F. Chouikha, "Attenuation characteristics of high rate home-networking PLC signals," *IEEE Trans. on Power Delivery*, vol. 17, no. 4, Oct. 2002, pp. 945-950.

[11] H. He, S. Cheng, Y. Zhang, J. Nguimbis, "Home network power-line communication signal processing based on wavelet packet analysis," *IEEE Trans. on Power Delivery*, vol. 20, no. 3, Jul. 2005, pp. 1879-1885.

[12] K. S. Surendran, H. Leung, "An analog spread-spectrum interface for power-line data communication in home networking," *IEEE Trans. on Power Delivery*, vol.20, no.1, pp.80,89, Jan. 2005

[13] H. Xu, S. Yang, "A loosely synchronous-coded OFDM system for power-line communications in home networks," *IEEE Trans. on Power Delivery*, vol. 21, no. 4, Oct. 2006, pp. 1912-1918.

[14] X. Lu, Y. Sun, I. H. Kim, "Reliable power line communication — A vehicle to smart home and smart energy," in *Proc. 2012 IEEE Intl. Conf. Consumer Electronics (ICCE)*, 13-16 Jan. 2012, pp. 86-87.

[15] R. Hashmat, P. Pagani, T. Chonavel, A. Zeddam, "A Time-Domain Model of Background Noise for In-Home MIMO PLC Networks," *IEEE Trans. on Power Delivery*, vol.27, no.4, Oct. 2012, pp. 2082-2089.

[16] C. Y. Park, K. H. Jung, W. H. Choi, "Coupling circuitary for impedance adaptation in power line communications using VCGIC," in *Proc. 12th IEEE Int. Symp. Power-Line Comm.*, 2008, pp. 293-298.

[17] H. M. Oh et al, "A coupler with transformer for impedance matching on MV power distribution line for BPLC," in *Proc. 12th IEEE Int. Symp. Power-Line Comm.*, 2008, pp. 409-412.

[18] F. Munoz, R. G. Carvajal, A. Torralba, L. G. Franquelo, E. Ramos, J. Pinilla, "ADAPT: mixed-signal ASIC for impedance adaptation in power line communications using fuzzy logic," in *Proc. 25th IEEE Ind. Electr. Soc. Conf.*, 1999, vol. 2, pp. 509-513.

[19] W. H. Choi, C. Y. Park, "A simple line coupler with adaptive impedance matching for power line communication," in *Proc. 11th IEEE Int. Symp. Power-Line Comm.*, 2007, pp. 187-191.

[20] M. P. Sibanda, P. A. Janse van Rensburg, H. C. Ferreira, "Passive, Transformerless Coupling Circuitry for Narrow-Band Power-Line Communications," in *Proc. 13th IEEE Int. Symp. Power-Line Comm.*, 2009, pp. 125-130.

[21] M. P. Sibanda, P. A. Janse van Rensburg, H. C. Ferreira, "Impedance Matching with Low-Cost Passive Components for Narrowband Power-Line Communications," in *Proc. 15th IEEE Int. Symp. Power-Line Comm.*, 2011, pp. 335-340.

[22] C. Bowick, *RF Circuit Design*, Howard W. Sams & Co., Inc., Indiana, 1982, pp. 67-97.

[23] J. B. Hagen, *Radio-Frequency Electronics: Circuits and Applications*, Cambridge University Press, 1996, pp. 9-17.

[24] M. P. Sibanda, "Economical L-C Coupling Circuits for Low-Voltage Power-line Communications," M.Eng Thesis, University of Johannesburg, March 2014, pp. 59, 94, available online at https://ujdigispace.uj.ac.za/handle/10210/10923

[25] H. C. Ferreira, H. M. Grové, O. Hooijen, and A. J. H. Vink, *Power Line Communication* (in *Wiley Encyclopaedia of Electrical and Electronics Engineering*), New York: Wiley, 1999, pp. 706-716.

[26] K. Dostert, *Powerline Communications*, Englewood Cliffs, NJ: Prentice-Hall, 2001, pp. 92, 241, 268.

[27] O. Hooijen, *Aspects of Residential Power Line Communications*, Aachen, Germany: Shaker Verlag, 1998, pp. 55, 63.

[28] R. Araneo, S. Celozzi, G. Lovat, F. Maradei, "Multi-Port Impedance Matching Technique for Power Line Communications," in *Proc. 15th IEEE Int. Symp. Power-Line Comm.*, 2011, pp. 96-101.

Petrus A. Janse van Rensburg was born in Pretoria, South Africa. He received the B.Sc degree in physics and the B.Ing degree in electrical engineering simultaneously from the Rand Afrikaans University, Johannesburg, South Africa, in 1994, where he also received the B.Sc.Hons (physics) and M.Ing (electrical) degrees in 1996 and 1997, respectively. In 2008, he was awarded the D.Ing (electrical) degree from the University of Johannesburg, South Africa.

Currently, he is Senior Lecturer at Walter Sisulu University, East London, South Africa. Previously, he was with Kendal Power Station and lectured at East London College. His research interests include integrated power electronics, power-line communications coupling and smart-grid applications. Dr. Janse van Rensburg is also the recipient of an IEEE Industry Applications Society prize paper award.

Mloyiswa P. Sibanda was born in Bulawayo, Zimbabwe. He received the B.Eng.Hons degree in electronic engineering from the National University of Science and Technology, Bulawayo, Zimbabwe, in 2003. He further received the M.Ing degree in electrical and electronic engineering from the University of Johannesburg, South Africa in 2014.

Currently, he is Lecturer at Walter Sisulu University, East London, South Africa. His research interests include power-line communications and the smart grid.

Hendrik C. Ferreira was born and educated in South Africa where he received the D.Sc (Eng.) degree from the University of Pretoria, South Africa, in 1980. In 1983, he joined the Rand Afrikaans University, Johannesburg, South Africa, (currently University of Johannesburg) where he was promoted to professor in 1989. He served two terms as Chairman of the Department of Electrical and Electronic Engineering at Rand Afrikaans University from 1994 to 1999.

His research interests include digital communications (especially power-line communications) and information theory (especially coding techniques). He has been principal adviser for more than 40 postgraduate students, of whom 10 have so far obtained a doctoral degree.

Prof. Ferreira is a past chairman of the Communications and Signal Processing Chapter of the IEEE South Africa section and the founding Chairman of the Information Theory Chapter. Between 1997 and 2005 he has been Editor-in-Chief of the Transactions of the South African Institute of Electrical Engineers. He has served as chairman of several conferences, including the recent 17th IEEE International Symposium on Power-Line Communications and its Applications (ISPLC 2013) that was held in Johannesburg, South Africa.